

THE EXTERNAL SHOCK MODEL OF GAMMA-RAY BURSTS: THREE PREDICTIONS AND A PARADOX RESOLVED

CHARLES D. DERMER,¹ MARKUS BÖTTCHER,^{1,2} AND JAMES CHIANG^{1,3,4}

Received 1998 October 15; accepted 1999 February 19; published 1999 March 9

ABSTRACT

In the external shock model, gamma-ray burst (GRB) emissions are produced by the energization and deceleration of a thin relativistic blast wave that interacts with the circumburst medium (CBM). We study the physical properties of an analytic function that describes temporally evolving GRB spectra in the limit of a smooth CBM with density $n(x) \propto x^{-\eta}$, where x is the radial coordinate. The hard-to-soft spectral evolution and the intensity-hardness correlation of GRB peaks are reproduced. We predict that (1) GRB peaks are aligned at high photon energies and lag at low energies according to a simple rule, that (2) temporal indices at the leading edge of a GRB peak display a well-defined shift with photon energy, and that (3) the change in the spectral index values between the leading and trailing edges of a GRB peak decreases at higher photon energies. The reason that GRBs are usually detected with νF_ν peaks in the 50 keV to several MeV range for detectors triggering on peak flux over a fixed time interval is shown to be a consequence of the inverse correlation of the peak flux and the duration of the radiation emitted by decelerating blast waves.

Subject headings: gamma rays: bursts — gamma rays: theory — radiation mechanisms: nonthermal

1. INTRODUCTION

The *BeppoSAX* results have revolutionized our understanding of gamma-ray bursts (GRBs) by opening a window on X-ray, optical, and radio afterglows that are delayed from the prompt X-ray and γ -ray emissions by several hours or more (see, e.g., Costa et al. 1997; Feroci et al. 1998; Piro et al. 1998; van Paradijs et al. 1997; Frail 1998). The decaying power-law, long-wavelength afterglows are compellingly explained as the emissions from a relativistic blast wave that decelerates and radiates through the process of sweeping up material from a uniform circumburst medium (CBM) (see, e.g., Paczyński & Rhoads 1993; Katz 1994; Mészáros & Rees 1997; Wijers, Rees, & Mészáros 1997; Tavani 1996). Afterglow behaviors that are more complicated than simple power laws may involve effects of extinction, self-absorption, scintillation, and CBM structure.

Mészáros & Rees (1993) proposed that the energy of a fireball's blast wave could be efficiently converted into radiation during the prompt gamma-ray-luminous phase of a GRB through the interaction of a blast wave with the CBM. In the external shock model, all GRB emissions are due to the effects of a single thin blast wave that interacts with the CBM. Because the directed kinetic energy of the blast wave is converted into nonthermal particle energy by sweeping up material from the CBM, the emitted radiation depends crucially on the density distribution of the CBM in the blast wave's path. Smoother GRB time profiles therefore represent more uniform CBMs, at least within the Doppler cone from which most of the detected GRB emissions originate. Conversely, erratic and spiky GRB time profiles represent blast-wave deceleration in highly textured CBMs (Dermer & Mitman 1999).

In a recent paper (Dermer, Chiang, & Böttcher 1999, hereafter DCB), we proposed a parametric description of the radiation observed from a spherically expanding blast wave that decelerates and is energized by sweeping up material from a smooth CBM. By “smooth,” we mean that the CBM density

distribution is adequately represented by the expression $n(x) = n_0 x^{-\eta}$, where x is the radial coordinate. In this limit, the deceleration of the blast wave produces a time profile that mimics the so-called fast rise, exponential decay (FRED) GRB light curves. Our *Ansatz* is that a smooth CBM produces an ideal FRED light curve. Conversely, a GRB that exhibits the classic FRED-type profile results from a fireball embedded within and expanding into a smooth CBM.

In this Letter, we make three quantitative predictions that can be tested using BATSE and *BeppoSAX* data from bright FRED-type GRB time profiles, although the predictions would be tested most thoroughly with a GRB telescope that is much more sensitive than BATSE and measures prompt GRB emission in the range between ≈ 1 keV and several MeV. In § 2, we describe the model equations derived in DCB. Spectral and temporal predictions are given analytically and described graphically for a model fireball with $\Gamma_0 = 300$. In § 3, we show that the reason that GRBs are usually observed with νF_ν peaks in the ~ 50 keV to several MeV range is understood when account is taken of blast-wave physics and the triggering properties of burst detectors.

2. ANALYTIC DESCRIPTION AND PREDICTIONS OF THE BLAST-WAVE MODEL

In DCB, a parameterization of the nonthermal synchrotron emission from a decelerating blast wave observed at time t and photon energy $\epsilon = h\nu/m_e c^2$ was proposed. The function is based on the analytic approach of Dermer & Chiang (1998) and the numerical results of Chiang & Dermer (1999), which were in turn based on the blast-wave physics developed by, e.g., Blandford & McKee (1976), Rees & Mészáros (1992), Piran & Shemi (1993), Mészáros & Rees (1993), Mészáros, Laguna, & Rees (1993), Waxman (1997), and Vietri (1997).

The deceleration of the relativistic blast wave is assumed to follow the expression $\Gamma(x) = \Gamma_0$ when $x \leq x_d$ and $\Gamma(x) = \Gamma_0(x/x_d)^{-g}$ when $x_d \leq x \leq x_d \Gamma_0^{1/g}$. Here Γ_0 is the initial bulk Lorentz factor of the blast wave, and the deceleration radius $x_d = 2.6 \times 10^{16} [(1 - \eta/3) E_{54} / (n_2 \Gamma_{300}^2)]^{1/3}$ cm. In this relation, the burst source emits $\partial E / \partial \Omega = 10^{54} E_{54} / (4\pi)$ ergs sr⁻¹, $\Gamma_0 \equiv 300 \Gamma_{300}$, and $n_2 = n_0 / (10^2 \text{ cm}^{-3})$. For simplicity, we consider only spherically symmetric blast waves. The parameter g spec-

¹ E. O. Hulburt Center for Space Research, Code 7653, US Naval Research Laboratory, Washington, DC 20375-5352.

² Department of Space Physics and Astronomy, Rice University, MS 108, 6100 South Main, Houston, TX 77005-1892.

³ JILA, University of Colorado, Campus Box 440, Boulder, CO 80309-0440.

⁴ NRL/NRC Resident Research Associate.

TABLE 1
STANDARD PARAMETERS FOR MODEL OF EVOLVING GRB SPECTRA

Parameter	Standard Value	Description
Γ_0	300	Baryon-loading parameter
q	10^{-3}	Equipartition term
g	2	Index of Γ evolution
$\partial E_0/\partial\Omega$	$10^{54}E_{54}/(4\pi)$	Total fireball energy released per unit solid angle (ergs sr $^{-1}$)
ν	$4/3$	Spectral index of rising portion of νL_ν spectrum
δ	0.2	Spectral index of falling portion of νL_ν spectrum
z	1	Cosmological redshift
n_0	10^2 cm^{-3}	Density at x_d
η	0	Index of density distribution

ifies the radiative regime, and $g \rightarrow (3 - \eta)/2$ and $g \rightarrow 3 - \eta$ in the adiabatic and radiative limits, respectively. The deceleration timescale $t_d = 9.7(1 + z)[(1 - \eta/3)E_{54}/(n_2\Gamma_{300}^8)]^{1/3}$ s.

The function proposed in DCB to model the blast-wave radiation has the broken power-law form

$$P(\epsilon, t) = 4\pi d_L^2 \nu F_\nu = \frac{(1 + \nu/\delta)P_p(t)}{[\epsilon/\epsilon_p(t)]^{-\nu} + (\nu/\delta)[\epsilon/\epsilon_p(t)]^\delta}, \quad (1)$$

where ν and δ are the νF_ν spectral indices at energies below and above the temporally evolving break energy $\epsilon_p(t)$, respectively. Expressions for $\epsilon_p(t) = \mathcal{E}_0[\Gamma(x)/\Gamma_0]^4(x/x_d)^{-\eta/2}$ and the time-varying amplitude $P_p(t) = \Pi_0[\Gamma(x)/\Gamma_0]^4(x/x_d)^{2-\eta}$ are given in DCB by equations (9) and (16), respectively. Equation (1) depends on the specification of the nine parameters listed in Table 1. The equipartition parameter $q = [\xi_H(r/4)]^{1/2}\xi_e^2$, where r is the compression ratio and ξ_H and ξ_e are the magnetic field and electron equipartition values, respectively (see eqs. [7] and [8] in DCB). The parameters ν , δ , g , η , and q are assumed to be independent of time. This assumption is obviously not true in general but is realized in the limit that high-quality broadband measurements from a bright FRED-type GRB are made over a sufficiently short observing time δt so that radiative cooling and magnetic field evolution timescales in the comoving frame are $\gg \Gamma\delta t/(1 + z)$.

The thick curves in Figure 1 show time profiles calculated at various observing energies ϵ , using the equations of the previous section. The thin curves show spectral indices cal-

culated between ϵ and 2ϵ . Here we show results for fireballs with $\Gamma_0 = 300$ that are located at redshift $z = 1$; other parameters are listed in Table 1. In this example, $t_d = 9.6(1 + z)$ s, and $\mathcal{E}_0 = 2.43/(1 + z)$. The model GRB light curves shown in Figure 1 display a rapid rise followed by a gentler decay that approaches a power-law afterglow behavior proportional to $t^{-1.52}$ (see eq. [22] in DCB) at late times $t \gg t_d$. The overall shape of the model light curves shown in Figure 1 resembles the characteristic FRED-type GRB light curve (see, e.g., Fishman & Meegan 1995). The model GRB represents a very bright BATSE GRB if located at $z = 1$ but would fall below BATSE detectability if located at $z \gtrsim 3$.

The analytic approximation used for the evolution of $\Gamma(x)$ gives spectral index curves that are constant when $t \leq t_d$. At later times, the blast-wave deceleration means that an observer measuring a photon spectrum over a fixed range of energies will sample photons that are produced at progressively higher energies in the blast wave's frame of reference. Because a nonthermal synchrotron spectrum from a power-law distribution of electrons with a low-energy cutoff is very hard at low energies and softens at higher energies, blast-wave deceleration produces the hard-to-soft spectral evolution observed in many GRB time profiles (Norris et al. 1986). If the observer is monitoring a GRB at $\epsilon \gtrsim \mathcal{E}_0$, the flux is brightest when $t \approx t_d$. As can be seen from Figure 1, the spectrum remains hard until $t \gtrsim t_d$, after which the blast wave begins to decelerate and the spectrum softens. Thus, the spectrum is hardest when it is most intense, accounting for the hardness-intensity correlation observed in GRB light curves (Golenetskii et al. 1983). If the blast wave produces short timescale variability by interacting with inhomogeneities in the CBM (Dermer & Mitman 1999), then the individual pulses in GRB profiles would likewise exhibit spectral hardening and subsequent softening, as generally observed in well-defined pulses of GRB light curves (Ford et al. 1995; Crider et al. 1998). The qualitative ability of the blast-wave model to explain these empirical trends has been pointed out previously by Panaitescu & Mészáros (1998).

We now propose three quantitative predictions to test the validity of this model. As is evident from Figure 1, the peak flux shifts to later times at lower photon energies. The peak times are given analytically by the expression

$$t_p(\epsilon) = t_d \max \left\{ 1, (1 + 2g)^{-1} \left[\left(\frac{\epsilon}{\mathcal{E}_0} \right)^{-(2g+1)/(4g+\eta/2)} + 2g \right] \right\} \quad (2)$$

(see also Chiang 1998). By plotting the times of a well-defined peak for a GRB measured over a large energy range, one tests the external shock model and constrains values of \mathcal{E}_0 and the exponent $(2g + 1)/(4g + \eta/2)$. The peak shifting will be more pronounced in GRBs with larger values of \mathcal{E}_0 .

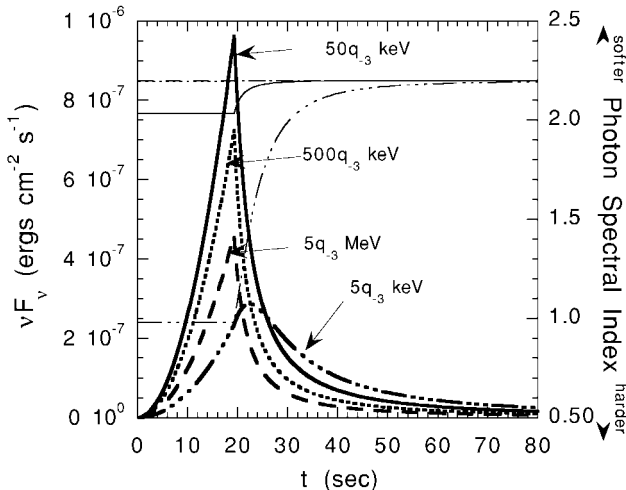


FIG. 1.—Light curves (thick lines) and spectral indices (thin lines) from a model GRB produced by a fireball with $\Gamma_0 = 300$ located at redshift $z = 1$. Other parameters are listed in Table 1.

Our second prediction is that the temporal indices of a pulse profile vary with photon energy according to the relation $\chi(\epsilon; t) = \partial \ln P(\epsilon, t) / \partial \ln t$. This yields a complicated analytic expression from equation (1), although it is easily calculated numerically. When $t < t_d$, however, the analytic form gives

$$P(\epsilon, t) = \Pi_0 \times \begin{cases} \left(1 + \frac{v}{\delta}\right) \left(\frac{\epsilon}{\epsilon_0}\right)^{-v} \left(\frac{t}{t_d}\right)^{2-\eta+\eta v/2} & \text{for } \epsilon \ll \epsilon_0, \\ \left(1 + \frac{\delta}{v}\right) \left(\frac{\epsilon}{\epsilon_0}\right)^{-\delta} \left(\frac{t}{t_d}\right)^{2-\eta-\eta\delta/2} & \text{for } \epsilon \gg \epsilon_0. \end{cases} \quad (3)$$

Thus, we predict that the temporal index χ changes from $2 - \eta(1 - v/2)$ at low energies to $2 - \eta(1 + \delta/2)$ at high energies. For a uniform CBM, there is no shift, and the temporal index $\chi = 2$. When $\eta \neq 0$, the relation between the temporal and spectral indices indicated by equation (3) implies the value of η .

As can also be seen from Figure 1, the spectral index is hardest at the leading edge of a GRB peak and softens at the trailing edge, with the change in the values of the spectral index decreasing toward higher photon energies. This prediction can be made quantitatively by taking the derivative of equation (1), giving the following result:

$$\alpha(\epsilon, t) = \frac{\partial \ln P(\epsilon, t)}{\partial \ln \epsilon} = \frac{v(y^{-v} - y^\delta)}{y^{-v} + (v/\delta)y^\delta} \quad (4)$$

for the νF_ν spectral index, where $y = \epsilon/\epsilon_p(t)$. The external shock model can be tested by plotting the energy-dependent variation of the spectral index across the peak of a GRB from equation (4).

Although the above equations provide a simple analytic characterization of the predictions of the external shock model, they depend crucially on the $\Gamma(x)$ -prescription noted above. Moreover, electron cooling is not taken into account in the analytic model. We used a numerical simulation code (Chiang & Dermer 1999) to determine the reliability of the analytic predictions. The results are shown in Figure 2 using the parameters of Table 1. Because the radiative regime g in the simulation depends on the magnetic field $H(G)$, the value of $\xi_H = H^2/[32\pi m_p c^2 n_0(r/4)]$ was adjusted until the bulk Lorentz factor approached the asymptotic behavior $\Gamma \propto x^{-2}$ in the deceleration phase. This occurred for $\xi_H \approx 3 \times 10^{-5}$. The injection spectrum of electrons is chosen to be proportional to $\gamma^{-3.4}$ in order to give an uncooled spectrum with $\delta = 0.2$. Electron cooling is seen to be important at high photon energies. The peak of the light curves at large photon energies occurs at $\approx t_d/2$, with a peak flux ≈ 2 times greater than the analytic estimate. We find that the qualitative trends of the predictions described above are reproduced in the detailed calculation. The analytic model can be used to confine the parameter range, but detailed fitting to data should employ the more accurate numerical simulations.

3. RESOLUTION OF THE RELATIVISTIC BEAMING/ νF_ν PEAK ENERGY PARADOX

Even if cosmic fireballs were produced with a narrow range of values of Γ_0 , their νF_ν peaks would be distributed over a wide range of photon energies since $\epsilon_0 \propto \Gamma_0^4$. It has therefore been something of a mystery to understand why GRBs are

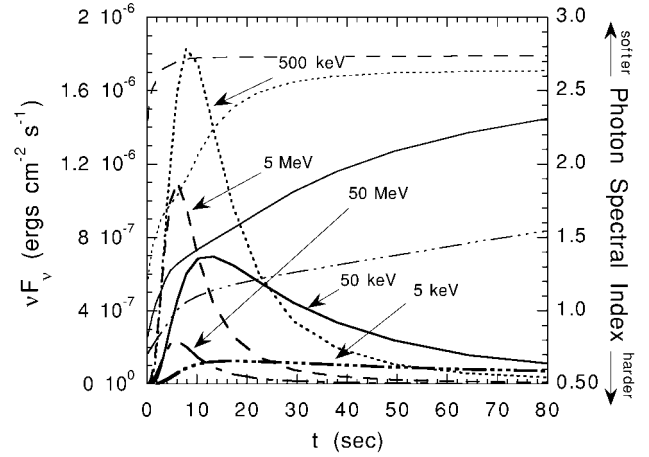


FIG. 2.—Numerical simulation results corresponding to the analytic model shown in Fig. 1 (see text for details). The equipartition between the energy in electrons, protons, and the magnetic field is assumed.

usually detected with νF_ν peaks in a narrow range of photon energies between ~ 50 keV and ~ 1 MeV (see, e.g., Malozzi et al. 1995; Piran & Narayan 1996) without requiring fine-tuning of the parameters. Brainerd's (1994) Compton attenuation model, for example, has been advanced to address this puzzle specifically. In contrast to GRBs, the nonthermal emissions in blazars are also thought to originate from relativistic outflows, yet they have νF_ν peaks in both their synchrotron and Compton components that range over 3 orders of magnitude or more in photon energy (see, e.g., von Montigny et al. 1995).

Using the spectral form proposed in DCB, we show how this paradox is resolved for a uniform CBM (the generalization to $\eta \neq 0$ is straightforward). Let us suppose that an instrument triggers on peak flux measured over the timescale Δt and over a narrow range of photon energies centered at ϵ_d . When the mean duration $t_p(\epsilon_d)$ of the fireball measured at ϵ_d is longer than Δt , then the detector triggers on peak flux. From the expressions for $\epsilon_p(t)$ and $P_p(t)$, we find that fireballs with $\Gamma_0 = \bar{\Gamma}_0 \approx 240[(1+z)\epsilon_d/(n_2^{3/8}q_{-3})]^{1/4}$ are observed with the peak of their νF_ν spectrum at photon energy ϵ_d at the moment when the received bolometric power is greatest (i.e., when $t = t_d$). Dirtier fireballs with $\Gamma_0 < \bar{\Gamma}_0$ produce a peak flux at ϵ_d that declines according to the relation $P_p(\epsilon_d, t_p) \propto \Gamma_0^{(4\delta+8/3)}$, which can be derived by inserting equation (2) into equation (1) in the limit $\epsilon_d \gg \epsilon_0$ (see also eq. [19] in DCB). Because $\delta > 0$, the peak flux therefore rapidly decreases with decreasing Γ_0 . Cleaner fireballs with $\Gamma_0 > \bar{\Gamma}_0$ are also more difficult to detect because, in this case, $P_p(\epsilon_d, t_p) \propto \Gamma_0^{2g-1-4/3}$ (cf. eq. [20] in DCB). In order to be observed at all, blast waves cannot be perfectly adiabatic, so that $g > 3/2$ and the peak flux detected with a GRB instrument decreases with increasing Γ_0 .

Cleaner fireballs are more difficult to detect than was indicated above because, when $t_d \ll \Delta t$, the detector triggers on fluence rather than on flux. The fluence F decreases with increasing Γ_0 according to $F \propto t_p P_p(\epsilon_d, t_p) \propto \Gamma_0^{g-1-2/3} \Gamma_0^{2g-1-4/3}$, using equation (2) and the expression for $\epsilon_p(t)$ with $\eta = 0$. Because of the emission properties of blast waves, detectors that trigger on a peak flux over a fixed time window will therefore be most sensitive to fireballs that have νF_ν peaks in the energy range of the detector. Hence, the discoveries of new classes of clean and dirty fireballs must employ analyses using varying time windows and energy ranges in the triggering criteria of a de-

tector, while taking into account the levels of the background radiation as discussed in DCB.

In separate work (Böttcher & Dermer 1999), we model the triggering properties of GRB detectors and show that, compared with the BATSE GRB trigger rate, the dirty fireball rate is poorly known because of selection biases against their detection. Observational analyses of *Ariel 5* X-ray data (Grindlay 1999; see discussion in DCB) provide the strongest available limit on the frequency of dirty fireballs. By contrast, the relative rate of clean fireballs is strongly constrained in the analysis of Böttcher & Dermer (1999) unless there is a strong anticorrelation between Γ_0 and q .

In summary, we have used a simple analytic description of the external shock model of GRBs to pose three predictions that can be tested by fitting equations (2)–(4) to high-quality data obtained with a GRB telescope that is sensitive in the ≈ 1

keV to several MeV range. Although we have employed a simple mathematical parameterization, detailed fits to data should use numerical simulations of the decelerating blast wave (see, e.g., Chiang & Dermer 1999 and Panaitescu & Mészáros 1998). We have also explained why detectors that trigger on peak flux are most sensitive to fireballs that produce νF_ν peaks in the 50 keV to several MeV range, resolving a long-standing puzzle in relativistic beaming models of GRBs.

We thank the referee for comments. The work of C. D. D. and M. B. was partially supported by the *Compton Gamma Ray Observatory* Guest Investigator Program. The work of J. C. was performed while he held a National Research Council/Naval Research Laboratory Associateship. C. D. D. acknowledges support from the Office of Naval Research.

REFERENCES

- Blandford, R. D., & McKee, C. F. 1976, *Phys. Fluids*, 19, 1130
 Böttcher, M., & Dermer, C. D. 1999, *ApJ*, submitted (astro-ph/9812059)
 Brainerd, J. J. 1994, *ApJ*, 428, 21
 Chiang, J. 1998, *ApJ*, 508, 752
 Chiang, J., & Dermer, C. D. 1999, *ApJ*, 512, 699
 Costa, E., et al. 1997, *Nature*, 387, 783
 Crider, A., et al. 1998, in preparation
 Dermer, C. D., & Chiang, J. 1998, *NewA*, 3, 157
 Dermer, C. D., Chiang, J., & Böttcher, M. 1999, *ApJ*, 513, 656 (DCB)
 Dermer, C. D., & Mitman, K. E. 1999, *ApJ*, 513, L5
 Feroci, M., et al. 1998, *A&A*, 323, L29
 Fishman, G. J., & Meegan, C. A. 1995, *ARA&A*, 33, 415
 Ford, L. A., et al. 1995, *ApJ*, 439, 307
 Frail, D. 1998, in *Fourth Huntsville Gamma-Ray Burst Symp.*, ed. C. A. Meegan, R. D. Preece, & T. M. Koshut (AIP: New York), 563
 Golenetskii, S. V., et al. 1983, *Nature*, 306, 451
 Grindlay, J. E. 1999, *ApJ*, 510, L710
 Katz, J. I. 1994, *ApJ*, 422, 248
 Mallozzi, R. S., Paciesas, W. S., Pendleton, G. N., Briggs, M. S., Preece, R. D., Meegan, C. A., & Fishman, G. J. 1995, *ApJ*, 454, 597
 Mészáros, P., Laguna, P., & Rees, M. J. 1993, *ApJ*, 415, 181
 Mészáros, P., & Rees, M. J. 1993, *ApJ*, 405, 278
 ———. 1997, *ApJ*, 476, 232
 Norris, J., et al. 1986, *ApJ*, 301, 213
 Paczyński, B., & Rhoads, J. 1993, *ApJ*, 418, L5
 Panaitescu, A., & Mészáros, P. 1998, *ApJ*, 492, 683
 Piran, T., & Narayan, R. 1996, in *Third Huntsville Gamma-Ray Burst Symp.*, ed. C. Kouveliotou, M. F. Briggs, & G. J. Fishman (New York: AIP), 233
 Piran, T., & Shemi, A. 1993, *ApJ*, 403, L67
 Piro, L., et al. 1998, *A&A*, 331, L41
 Rees, M. J., & Mészáros, P. 1992, *MNRAS*, 258, 41P
 Tavani, M. 1996, *Phys. Rev. Lett.*, 76, 3478
 van Paradijs, J., et al. 1997, *Nature*, 386, 686
 Vietri, M. 1997, *ApJ*, 478, L9
 von Montigny, C., et al. 1995, *ApJ*, 440, 525
 Waxman, E. 1997, *ApJ*, 485, L5
 Wijers, R. A. M. J., Rees, M. J., & Mészáros, P. 1997, *MNRAS*, 288, L51